Plastic Phase Transitions in *N*-Ethyl-*N*-methylpyrrolidinium Bis(trifluoromethanesulfonyl)imide

Wesley A. Henderson,[†] Victor G. Young, Jr.,[‡] Stefano Passerini,[§] Paul C. Trulove,*[,†] and Hugh C. De Long[||]

Department of Chemistry, U.S. Naval Academy, 572 M. Holloway Road, Annapolis, Maryland 21402, X-ray Crystallographic Laboratory, Department of Chemistry, University of Minnesota, S146C Kolthoff Hall, 207 Pleasant Street SE, Minneapolis, Minnesota 55455, ENEA, Casaccia Research Center, Via Anguillarese 301, 00060 Rome, Italy, and Air Force Office of Scientific Research, 4015 Wilson Boulevard, Arlington, Virginia 22203

Received August 26, 2005. Revised Manuscript Received December 20, 2005

The salt *N*-ethyl-*N*-methylpyrrolidinium bis(trifluoromethanesulfonyl)imide ($PYR_{12}TFSI$) undergoes several solid−solid phase transitions before melting at 91 °C. At −120 °C, the crystal structure consists of ordered ions (phase IV). After the solid−solid phase transition at −85 °C, however, all of the PYR_{12}^+ and $TFSI^-$ ions become disordered, forming a plastic crystalline phase (phase III). We report here the $PYR_{12}TFSI$ phase III and IV structures determined from single-crystal diffraction data using the same crystal. The two structures are compared to elucidate the mechanism of the phase transition and gain a greater understanding of disordering modes of ions in the solid state.

Introduction

Solid−solid phase transitions of salts from an ordered phase to disordered crystalline phases, that is, plastic crystalline phases, in which some or all of the ions gain orientational, rotational, and perhaps even translational degrees of freedom are a topic of great interest for both the development of a fundamental understanding of physical phenomena in condensed matter and more applied interests such as lithium battery technologies,[1] ferroelectrics,[2] and explosives.[3] *N*-Methyl-*N*-alkylpyrrolidinium (PYR_{1R}^+ where the subscript $R = 1$ for methyl, 2 for ethyl, etc.) salts with $N(SO_2CF_3)_2^-$ ($TFSI^-$) and other anions have been reported and extensively studied by MacFarlane's group.[4] Some of these salts have plastic crystalline phases, whereas others have subambient melting points (mp's) resulting in their classification as room-temperature ionic liquids.[5] For most cases, it is still unclear which ions become disordered in the plastic crystalline phases, how this disordering occurs, and how this, in turn, influences the mp of a salt. Some limited work has been reported examining the phase transitions of pyrrolidinium salts.[2,6] A detailed understanding of the crystal packing arrangement of ions in a given salt and the ion disordering mechanisms may help explain why the mp's of $PYR_{1R}TFSI$ salts vary dramatically, that is, mp's with $R =$ 1−4 are 135, 91, 12, and −3 °C, respectively.[7] Here, we report the crystal structures of the low-temperature ordered $PYR_{12}TFSI$ crystalline phase (phase IV) and the first PYR_{12}-TFSI disordered plastic crystalline phase (phase III). In the latter, all of the ions are disordered, although the crystal ionic packing is similar to the phase IV ordered structure. The phases have been numbered using the standard convention, with phase I being the phase present just prior to the fusion transition with subsequent phases numbered with decreasing temperature.

* To whom correspondence should be addressed. E-mail: trulove@usna.edu.
[†] U.S. Naval Academy.
[‡] University of Minnesota.
[§] ENEA.
[||] U.S. Air Force Office of Scientific Research.

(1) (a) MacFarlane, D. R.; Huang, J.; Forsyth, M. *Nature* **1999**, *402*, 792. (b) MacFarlane, D. R.; Forsyth, M. *Adv. Mater.* **2001**, *13*, 957. (c) Alarco, P.-J.; Abu-Lebdeh, Y.; Armand, M. *Solid State Ionics* **2004**, *175*, 717.

(2) (a) Bednarska-Bolek, B.; Jakubas, R.; Medycki, W.; Nowak, D.; Zaleski, J. *J. Phys.: Condens. Matter* **2002**, *14*, 3129. (b) Medycki, W.; Świergiel, J.; Hołderna-Natkaniec, K.; Jurga, K.; Jakubas, R. *Solid State Nucl. Magn. Res.* **2004**, *25*, 129. (c) Jakubas, R.; Bednarska-Bolek, B.; Zaleski, J.; Medycki, W.; Holderna-Natkaniec, K.; Zielinski, P.; Galazka, M. *Solid State Sci.* **2005**, *7*, 381.

(3) (a) Sorescu, D. C.; Thompson, D. L. *J. Phys. Chem. A* **2001**, *105*, 720. (b) Coffey, C. S.; Sharma, J. *Phys. Rev. B* **1999**, *60*, 9365.

(4) (a) MacFarlane, D. R.; Meakin, P.; Sun, J.; Amini, N.; Forsyth, M. *J. Phys. Chem. B* **1999**, *103*, 4164. (b) Hill, A. J.; Huang, J.; Efthimiadis, J.; Meakin, P.; Forsyth, M.; MacFarlane, D. R. *Solid State Ionics* **2002**, *154*−*155*, 119. (c) Golding, J.; Hamid, N.; MacFarlane, D. R.; Forsyth, M.; Forsyth, C.; Collins, C.; Huang, J. *Chem. Mater.* **2001**, *13*, 558. (d) Forsyth, S. A.; Batten, S. R.; Dai, Q.; MacFarlane, D. R. *Aust. J. Chem.* **2004**, *57*, 121. (e) Pringle, J. M.; Golding, J.; Forsyth, C. M.; Deacon, G. B.; Forsyth, M.; MacFarlane, D. R. *J. Mater. Res.* **2002**, *12*, 3475. (f) Golding, J.; Forsyth, S.; MacFarlane, D. R.; Forsyth, M.; Deacon, G. B. *Green Chem.* **2002**, *4*, 223. (g) MacFarlane, D. R.; Forsyth, S. A.; Golding, J.; Deacon, G. B. *Green Chem.* **2002**, *4*, 444. (h) Forsyth, C. M.; MacFarlane, D. R.; Golding, J. J.; Huang, J.; Sun, J.; Forsyth, M. *Chem. Mater.* **2002**, *14*, 2103. (i) Sun, J.; MacFarlane, D. R.; Forsyth, M. *J. Mater. Chem.* **2001**, *11*, 2940. (j) MacFarlane, D. R.; Golding, J.; Forsyth, S.; Forsyth, M.; Deacon, G. B. *Chem. Commun.* **2001**, 1430.

(5) Wasserscheid, P., Welton, R., Eds. *Ionic Liquids in Synthesis*; Wiley-VCH: Weinheim, Germany, 2003.

(6) (a) Misaki, S.; Kashino, S.; Haisa, M. *Acta Crystallogr., Sect. C* **1989**, *45*, 917. (b) Ono, H.; Ishimaru, S.; Ikeda, R.; Ishida, H. *Bull. Chem. Soc. Jpn.* **1999**, *72*, 2049. (c) Ishida, H.; Furukawa, Y.; Sato, S.; Kashino, S. *J. Mol. Struct.* **2000**, *524*, 95. (d) Adebahr, J.; Forsyth, M.; MacFarlane, D. R. *Electrochim. Acta* **2005**, *50*, 3853. (e) Adebahr, J.; Seeber, A. J.; MacFarlane, D. R.; Forsyth, M. *J. Appl. Phys.* **2005**, *97*, 093904.

(7) Henderson, W. A.; Passerini, S. *Chem. Mater.* **2004**, *16*, 2881.

10.1021/cm051936f CCC: $33.50
Published on Web 01/28/2006

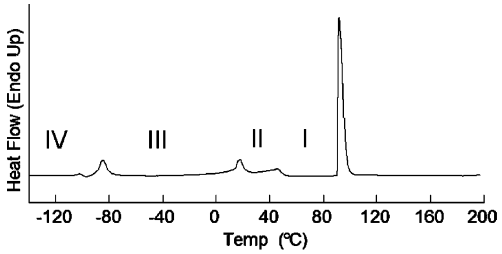

Figure 1. DSC heating trace of $PYR_{12}TFSI$.

Table 1. Crystal and Refinement Data

	phase IV	phase III
chemical formula	$C_9H_{16}F_6N_2O_4S_2$	$C_9H_{16}F_6N_2O_4S_2$
fw	394.36	394.36
wavelength (Å)	0.71073	0.71073
crystal system	monoclinic	triclinic
space group	$P2_1/n$	P-1
a (Å)	13.099(3)	8.5425(14)
b (Å)	14.454(3)	9.6978(16)
c (Å)	16.987(4)	11.2219(18)
α (deg)	90	88.487(3)
β (deg)	97.546(4)	73.119(3)
γ (deg)	90	68.294(3)
V (Å^3)	3188.5(13)	823.1(2)
Z	8	2
T (K)	153(2)	213(2)
ρ_{calc} (g cm^{-3})	1.643	1.591
μ (mm^{-1})	0.415	0.402
crystal size (mm)	0.40 × 0.16 × 0.06	0.40 × 0.16 × 0.06
F(000)	1616	404
$2\theta_{max}$ (deg)	25.13	25.05
N (R_{int})	5657 (0.0470)	2901 (0.0360)
N [$I > 2\sigma(I)$]	4646	1832
R_1,[a] wR_2[b] [$I > 2\sigma(I)$]	0.0587, 0.1549	0.0864, 0.2658
R_1,[a] wR_2[b] (all data)	0.0718, 0.1613	0.1166, 0.2931
GOF[c]	1.051	1.097
$\Delta e_{min,max}$ (e Å^{-3})	−0.367, 0.899	−0.398, 0.523

[a] $R_1 = \sum||F_o| - |F_c||/\sum|F_o|$. [b] $wR_2 = [\sum[w(F_o^2 - F_c^2)^2]/\sum[w(F_o^2)^2]]^{1/2}$. [c] GOF $= [\sum[w(F_o^2 - F_c^2)^2]/(n - p)]^{1/2}$.

Results and Discussion

$PYR_{12}TFSI$ Thermal Behavior. The DSC thermal behavior of $PYR_{12}TFSI$ has been reported in detail elsewhere,[4a,b] but is briefly reviewed here for clarity. In the solid state, the salt has several crystalline phases, that is, IV, III, II, and I, with transition temperatures (T_{IV-III}, T_{III-II}, and T_{II-I}) at −85, 17, and 45 °C, respectively. $PYR_{12}TFSI$ melts (T_{I-L}) at 91 °C (Figure 1). Melting occurs in a sudden step, rather than gradually. The T_{II-I} transition appears to be second order, whereas the T_{III-II} and T_{IV-III} transitions have both first- and second-order character. Note that a small peak at −102 °C prior to the T_{IV-III} peak at −85 °C indicates that a fourth solid−solid phase transition may also occur (Figure 1). We have neglected this in the following discussion because it is of low energy.

$PYR_{12}TFSI$ Phase IV Structure. Crystal and refinement data for the phase IV structure are given in Table 1. The asymmetric unit of the $PYR_{12}TFSI$ crystal structure at −120 °C contains two PYR_{12}^+ cations and two $TFSI^-$ anions (Figure 2). All of the ions are ordered. Both of the $TFSI^-$ anions adopt the low-energy C_2 conformation.[8] The cations adopt an envelope (C_S) conformation.

(8) (a) Johansson, P.; Gejji, S. P.; Tegenfeldt, J.; Lindgren, J. *Electrochim. Acta* **1998**, *43*, 1375. (b) Arnaud, R.; Benrabah, B.; Sanchez, J.-Y. *J. Phys. Chem.* **1996**, *100*, 10882. (c) Xue, L.; Padgett, C. W.; DesMarteau, D. D.; Pennington, W. T. *Solid State Sci.* **2002**, *4*, 1535.

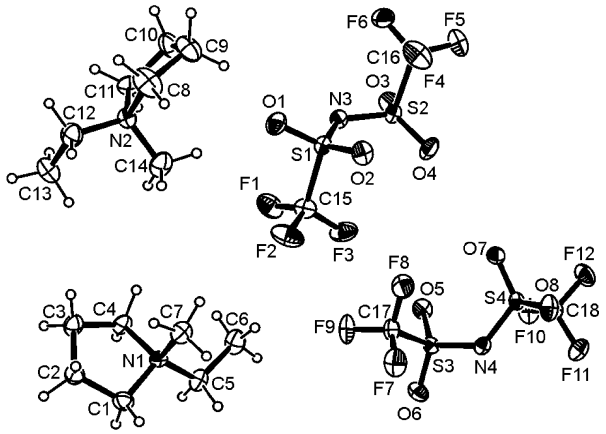

Figure 2. Asymmetric unit of the $PYR_{12}TFSI$ phase IV structure at −120 °C (30% thermal ellipsoids).

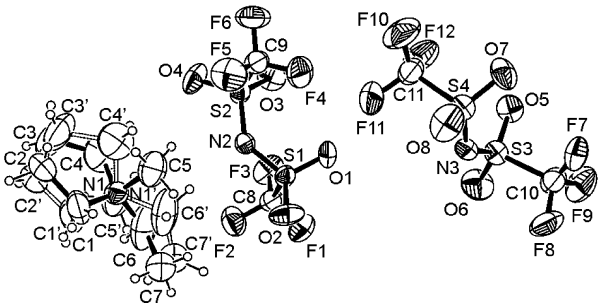

Figure 3. Asymmetric unit of the $PYR_{12}TFSI$ phase III structure at −60 °C (30% thermal ellipsoids) (anions are disordered by symmetry − not shown).

$PYR_{12}TFSI$ Phase III Structure. Crystal and refinement data for the phase III structure are given in Table 1. The unit cell of the phase III structure contains $^1/_4$ of the contents of the phase IV structure. In the phase III structure, all of the ions are disordered. The asymmetric unit of the PYR_{12}-$TFSI$ crystal structure at −60 °C contains one PYR_{12}^+ cation and two-half $TFSI^-$ anions (Figure 3). The PYR_{12}^+ cation is assumed to be 50:50 disordered about its long axis defined by the N1 nitrogen and the centroid of the C2/C3 carbons. Each half $TFSI^-$ anion is located on a unique inversion center. The anion disorder is not shown in Figure 3 because it originates from a symmetry operation. Requisite restraints and constraints were imposed; the number of restraints exceeds parameters. Some bond distances still fall outside the normal ranges even after employing these restraints. The phase transition occurring between the ordered monoclinic phase IV and disordered triclinic phase III is quite drastic. The ratio of the two twin components is also different. While phase III had a 2:1 ratio, phase IV had a 7:1 ratio. Perhaps this means that, given enough time and annealing, a single crystal could be produced.

The dramatic increase in thermal disorder of the atoms is evident from the difference in the anisotropic displacements of the two structures. In addition, both the PYR_{12}^+ cations and $TFSI^-$ anions in phase III appear to possess rotational disorder. The conformers of the ions in the two different disorder models for the cations and anions are shown in Figure 4a. It is not possible to superimpose the two structures for the cations and anions, respectively (Figure 4b). This indicates that, in addition to rotation about a central axis for

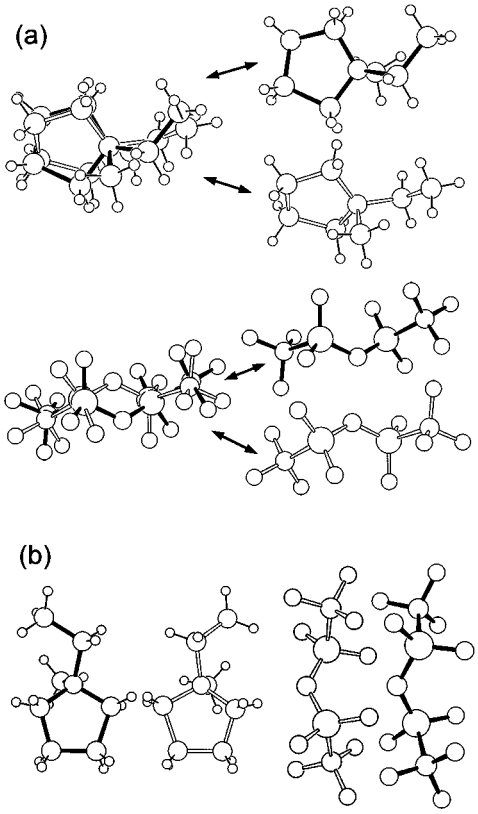

Figure 4. (a) Cation and anion disorder and (b) comparison of the disordered ion conformations in the $PYR_{12}TFSI$ phase III structure at −60 °C.

portions of the ions, the conformations of the ions also change. The PYR_{12}^+ cations rotate about an axis through the N1 nitrogen and the centroid between the C2 and C3 carbons (the ring flips). This is clear because the methyl group attached to the nitrogen of the cation has opposite orientation in the two conformers. The ethyl group also undergoes a conformation change. This minimizes the additional space required for the two conformers in the cage created by the neighboring anions (the two conformers occupy approximately the same volume). The $TFSI^-$ anions also rotate about a central axis through the two sulfurs, along with rotations of the SO_2CF_3 groups. This changes the orientation of the nitrogen and oxygens, but the SCF_3 groups have approximately the same positioning (although the CF_3 groups are rotated about the C_3 axis). The $TFSI^-$ anions in both conformers have C_2 symmetry. Again, this form of disordering minimizes the additional volume necessary for the ordered to disordered transition in the cage created by the neighboring cations. This $TFSI^-$ anion disordering mechanism has been recently reported by us in a supercooled plastic crystalline phase of Et_4NTFSI.[9]

Pyrrolidinium cations have two low-energy, twisted (C_2) and envelope (C_S), ring conformations.[10] The ordered PYR_{12}^+ cations in the phase IV $PYR_{12}TFSI$ structure have the envelope (C_S) conformation as is also found in the ordered $PYR_{11}I$ and $PYR_{11}TFSI$ crystal structures.[4c,h] The model for

(9) Henderson, W. A.; Herstedt, M.; Young, V. G., Jr.; Passerini, S.; De Long, H. C.; Trulove, P. C. *Inorg. Chem.*, in press.
(10) (a) Ishida, H.; Furukawa, Y.; Sato, S.; Kashino, S. *J. Mol. Struct.* **2000**, *524*, 95. (b) Bednarska-Bolek, B.; Jakubas, R.; Medycki, W.; Nowak, D.; Zaleski, J. *J. Phys.: Condens. Matter* **2002**, *14*, 3129.

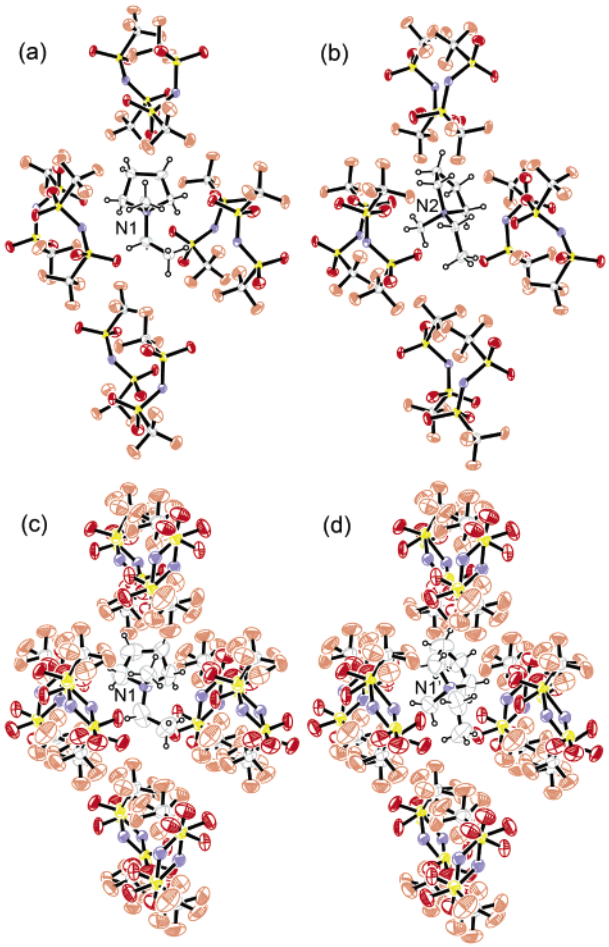

Figure 5. Comparison of the anion packing around a cation in the ordered $PYR_{12}TFSI$ phase IV structure at −120 °C: (a) cation with N1 nitrogen, (b) cation with N2 nitrogen and disordered $PYR_{12}TFSI$ phase III structure at −60 °C, (c) cation with N1 nitrogen (the other cation is not shown), and (d) cation with N1′ nitrogen (the other cation is not shown) (30% thermal ellipsoids).

the disordered PYR_{12}^+ cations used in the phase III PYR_{12}-$TFSI$ structure consists of two cations, both with envelope (C_S) conformations. The ring cations, however, have large thermal parameters and closely spaced carbons. Thus, twisted (C_2) conformers cannot be excluded as alternatives for the proposed model.

It is evident that the ion disorder in the phase III structure must be dynamic in nature, rather than static because the two reported structures originate from the same crystal. There must, therefore, be transitions between the two conformations found for the cations and anions, respectively. At −60 °C, however, the lifetime of the ions in the transition states may be much shorter than that of the ions in one of the two disordered conformations. Thus, only the two low-energy states are observed by crystallography at −60 °C. As the temperature increases, the barriers for these transition states decrease and the ions begin to flip between the states more rapidly. This explains why the high angle diffraction data rapidly drop off as the temperature increases above −60 °C.

Besides the disordering of the ions, just how different are the ordered phase IV and disordered phase III structures? Figure 5 shows the anion crystal packing around a PYR_{12}^+ cation in the two structures. It is immediately evident that the cations in both structures are surrounded by eight $TFSI^-$

anions. In the ordered phase IV structure, there are two separate cations with different anion environments (Figure 5a and b). In the disordered phase III structure, however, there is a single disordered cation with two orientations. An examination of the disordered anions around these two cation orientations suggests that the anion environment is identical to that found in the ordered state (Figure 5c and d). The two different cation sites in the phase IV structure are transposed into a single site in the phase III structure by the ion disorder. The close packing of the ions results in holes for the counterions of a specific size and shape. The disordered structure implies that both the cations and the anions are flipping between two orientations with different conformations. It may be that this occurs via a "wave- or cascade-mechanism" through the crystal; that is, as an ion switches its orientation and conformation, it induces a corresponding transformation in all of its neighboring ions due to steric and other interactions. The disorder transformation will thus progress through the crystal like a wave.

The unit cell of the phase III structure has only $^1/_4$ as many ions as the phase IV structure. Quadrupling the calculated unit cell volume for the disordered phase III structure gives a volume of 3292.5 Å^3 or an increase of 104.0 Å^3 relative to the ordered phase IV structure. Thus, the disordering mechanism adopted by the cations and anions in the phase III structure requires only a 3% increase in volume (from −120 to −60 °C) from the phase IV structure. This and the similar ionic packing explain the relative low energy of the T_{IV-III} transition despite the large increase in ion disorder.

Conclusion

Crystal structures for the ordered phase IV and disordered phase III of $PYR_{12}TFSI$ have been determined from single-crystal diffraction data. The two structures are nearly identical in the packing of the ions, but in the latter structure all of the ions become disordered. This solid−solid phase transition is of low energy and requires only a 3% change in volume. The $TFSI^-$ anions undergo a $C_2 \leftrightarrow C_2$ disordering mode that clearly is one of the standard disordering mechanisms for these anions in the solid state. The information reported regarding the solid−solid phase transition to a disordered phase and the mechanisms for the ion disordering might prove useful for explaining the low melting temperatures of many salts forming ionic liquids.

Experimental Section

$PYR_{12}TFSI$ Preparation. The $PYR_{12}TFSI$ salt was prepared by a metathesis reaction between $PYR_{12}I$ and LiTFSI in deionized water. $PYR_{12}I$ was prepared by combining equimolar amounts of 1-methylpyrrolidine and iodoethane in ethyl acetate. The reaction is very exothermic. Both $PYR_{12}I$ and LiTFSI are highly soluble in water, but upon mixing the two solutions, the white solid $PYR_{12}TFSI$ salt crystallizes rapidly. $PYR_{12}TFSI$ was purified by melting the salt in hot deionized water, and allowing the solution to cool and the salt to crystallize before pouring off the water. This was repeated five times. Single crystals were produced as the hot aqueous solutions slowly cooled.

Thermal Characterization. The DSC heating trace was obtained using a TA model 2910 differential scanning calorimeter (DSC). The salt was dried under vacuum for 24 h at 80 °C and then a further 4 h at 120 °C. A hermetically sealed Al pan with the salt was prepared in a dry room (<0.1% relative humidity). The sample was cooled at 5 °C/min from room temperature to −140 °C and then heated at 5 °C/min to 200 °C.

Crystal Structure Determination. A larger crystal was cut from a long needle and partially dissolved in a water/ethanol mixture to remove deformation around the cleaved portion. The crystal was then cooled from room temperature to −60 °C at 1 °C min^{-1}. Diffraction data were collected to determine the phase III structure. The same crystal was then further cooled to −120 °C at 1 °C min^{-1}. Diffraction data were again collected to determine the phase IV structure.

A preliminary set of cell constants was calculated from reflections harvested at −60 °C from four sets of 50 frames containing 327 reflections. Three twin components were indexed. The reference component was relatively large, while the other two were small. One twin component is a true nonmerohedral twin, while the other appears to be randomly oriented.[11] The nonmerohedral twin law (by rows) is [1 0 0/0 −1 0/−0.335 0 −1], which is a 180° rotation about (100). The twin law of the randomly oriented twin (by rows) is [0.479 0.793 0.103/0.769 −0.421 0.580/0.628 −0.405 −0.744], which is a 147.4° rotation around an irrational direct axis (1.000 0.494 0.223). Because of the random orientation of the third twin component, it was not included in the integration. A handful of reflections were removed prior to the final set of least squares.

A preliminary set of cell constants was calculated from reflections harvested at −120 °C from four sets of 50 frames containing 223 reflections. Two twin components were indexed. The ratio of masses for both is approximately 2:1. At least one randomly oriented satellite was indexed, but because it was deemed not to interfere with the pair, it was not included in the integration phase.[11] The nonmerohedral twin law (by rows) is [−1 0.026 −0.026/0 −0.149 −0.851/0 −1.149 −0.149], which is a 180° rotation about a direct axis (0 −1 1).

Final cell constants were calculated from strong reflections from the actual data collection after integration (SAINT).[12] The intensity data were corrected for absorption and decay (TWINABS).[13] Both structures were solved and refined using Bruker SHELXTL.[14] The SHELX HKLF 5 data for both phases III and IV were treated with Strip Redundant V1.3.[15] In like manner, the data for phase IV were treated with SysAbsFilter V1.3.[16] The space groups were determined on the basis of systematic absences and intensity statistics. A direct-methods solution was calculated, which provided most non-hydrogen atoms from the E-map. Full-matrix least squares/difference Fourier cycles were performed, which located the remaining non-hydrogen atoms. All non-hydrogen atoms were refined with anisotropic displacement parameters. All hydrogen atoms were placed in ideal positions and refined as riding atoms with relative isotropic displacement parameters. Schematics of the structures were drawn using ORTEP-3 and Mercury 1.4.

Acknowledgment. W.A.H. is indebted to the National Science Foundation for the award of a fellowship (International Research Fellowship Program 0202620), and P.C.T. gratefully

(11) Sheldrick, G. *CELL_NOW beta test V3*; University of Gottingen, 2004.
(12) *SAINT V6.2*; Bruker Analytical X-ray Systems, Madison, WI, 2001.
(13) TWINABS V1.07: (a) Sheldrick, G. University of Gottingen, 2004. (b) Blessing R. *Acta Crystallogr., Sect. A* **1995**, *51*, 33.
(14) *SHELXTL V6.12*; Bruker Analytical X-ray Systems, Madison, WI, 2000.
(15) Brennessel, W. W.; Young, V. G., Jr. *Strip Redundant V1.3, A program for removing redundant reflections from SHELX HKLF 5 type data*; 2003, unpublished.
(16) Brennessel, W. W.; Young, V. G., Jr. *SysAbsFilter V1.3, A program for removing systematically absense reflections from SHELX HKLF 5 type data*; 2003, unpublished.

acknowledges the financial support of the Naval Academy Research Council (NARC). Portions of this work were funded by the U.S. Air Force Office of Scientific Research. Any opinions, findings, and conclusions or recommendations expressed in this material are those of the author(s) and do not necessarily reflect the views of the National Science Foundation or U.S. Air Force.

Supporting Information Available: X-ray crystallographic data files for the phase III and IV structures of $PYR_{12}TFSI$ (CIF). This material is available free of charge via the Internet at http://pubs.acs.org.

CM051936F